Geophysical Research Letters

RESEARCH LETTER
10.1029/2022GL101249

Antarctic Ice-Sheet Meltwater Reduces Transient Warming and Climate Sensitivity Through the Sea-Surface Temperature Pattern Effect

Yue Dong[1,2], Andrew G. Pauling[3], Shaina Sadai[4,5], and Kyle C. Armour[3,6]

[1]Lamont-Doherty Earth Observatory, Columbia University, Palisades, NY, USA, [2]Cooperative Programs for the Advancement of Earth System Science, University Corporation for Atmospheric Research, Boulder, CO, USA, [3]Department of Atmospheric Sciences, University of Washington, Seattle, WA, USA, [4]Union of Concerned Scientists, Cambridge, MA, USA, [5]Department of Geosciences, University of Massachusetts, Amherst, MA, USA, [6]School of Oceanography, University of Washington, Seattle, WA, USA

Abstract Coupled global climate models (GCMs) generally fail to reproduce the observed sea-surface temperature (SST) trend pattern since the 1980s. The model-observation discrepancies may arise in part from the lack of realistic Antarctic ice-sheet meltwater input in GCMs. Here we employ two sets of CESM1-CAM5 simulations forced by anomalous Antarctic meltwater fluxes over 1980–2013 and through the 21st century. Both show a reduced global warming rate and an SST trend pattern that better resembles observations. The meltwater drives surface cooling in the Southern Ocean and the tropical southeast Pacific, in turn increasing low-cloud cover and driving radiative feedbacks to become more stabilizing (corresponding to a lower effective climate sensitivity). These feedback changes can contribute as substantially as ocean heat uptake efficiency changes in reducing the global warming rate. Accurately projecting historical and future warming thus requires improved representation of Antarctic meltwater and its impacts.

Plain Language Summary Observations have shown surface cooling in the Southern Ocean and the tropical southeast Pacific over the last four decades. However, global climate models generally struggle to reproduce this pattern. The model-observation mismatch has been proposed to partly arise from the fact that models lack in representation of realistic Antarctic ice-sheet meltwater input to the Southern Ocean. Here we revisit two sets of simulations with meltwater fluxes and examine the impact of meltwater input on global warming and the global energy budget. We find that accounting for meltwater input slows global warming and produces a surface warming pattern closer to recent observations. The reduced global warming rate is caused by both more efficient ocean heat uptake and stronger radiative feedbacks (more efficient radiative damping to space) that are associated with changes in the surface warming pattern. These results indicate a critical impact of Antarctic meltwater on the global climate that has been missed in current climate models.

Key Points:

- Accounting for Antarctic meltwater input in a global climate model reduces the global warming rate and produces a warming pattern closer to the observed
- Antarctic meltwater impacts not only the Southern Ocean, but also the tropics via teleconnections
- The reduced global warming rate is driven by changes in both ocean heat uptake efficiency and radiative feedbacks

Supporting Information:

Supporting Information may be found in the online version of this article.

Correspondence to:

Y. Dong,
yd2644@columbia.edu

Citation:

Dong, Y., Pauling, A. G., Sadai, S., & Armour, K. C. (2022). Antarctic ice-sheet meltwater reduces transient warming and climate sensitivity through the sea-surface temperature pattern effect. *Geophysical Research Letters*, *49*, e2022GL101249. https://doi.org/10.1029/2022GL101249

Received 12 SEP 2022
Accepted 4 DEC 2022

1. Introduction

The observed sea-surface temperature (SST) trend pattern since about 1979 is characterized by a strengthened east-west gradient in the tropical Pacific and a north-south hemispheric asymmetry: the tropical western Pacific and the Arctic have warmed while the tropical southeast Pacific and the Southern Ocean have cooled (Armour et al., 2016; England et al., 2014; Watanabe et al., 2021; Wills et al., 2022). The observed surface cooling in the Southern Ocean has been accompanied by an insignificant trend in Antarctic sea-ice extent (Fan et al., 2014; Parkinson, 2019), broad surface freshening (De Lavergne et al., 2014; Durack, 2015) and sub-surface warming (Armour et al., 2016; Gille, 2008). Yet. all these observed regional features are generally missed in global-climate model (GCM) simulations driven by historical forcings (Chung et al., 2022; Kostov et al., 2018; Luo et al., 2018; Roach et al., 2020; Seager et al., 2022; Wills et al., 2022), with many models also overestimating the global-mean warming rate over this period (Jiménez-de-la Cuesta & Mauritsen, 2019; Nijsse et al., 2020; Tokarska et al., 2020).

Various hypotheses have been put forward to explain the observed changes and model-observation discrepancies, including natural variability in the Pacific Ocean (Watanabe et al., 2021) or in the Atlantic Ocean (McGregor et al., 2018) and model biases in various forcings and forced responses (Seager et al., 2019; Takahashi & Watanabe, 2016), as summarized in recent studies (Andrews et al., 2022; Lee et al., 2022; Wills et al., 2022). One of the leading hypotheses for the observed changes in the Southern Ocean is freshwater input from the melt of

the Antarctic ice sheet and ice shelves (referred to here as Antarctic "meltwater"). The fact that the current generation of GCMs is unable to represent Antarctic meltwater fluxes may explain some of the model-observation discrepancies in the Southern Ocean. Indeed, numerous studies have shown that adding an Antarctic meltwater flux in GCMs can produce anomalous surface cooling, subsurface warming, and sea-ice expansion around Antarctica, owing to an increase in upper ocean stratification, reducing the vertical heat flux from the relatively warm subsurface waters below (Armour et al., 2016; Bintanja et al., 2013; Bronselaer et al., 2018; Kirkman & Bitz, 2011; Ma & Wu, 2011; Park & Latif, 2019; Pauling et al., 2016; Purich et al., 2018; Rye et al., 2020; Sadai et al., 2020; Schloesser et al., 2019; Swart & Fyfe, 2013). Although the amount of Antarctic meltwater input needed to cause significant changes in the Southern Ocean is highly model dependent (e.g., Bintanja et al., 2013; Pauling et al., 2016; Swart & Fyfe, 2013), meltwater forcing brings projected Southern Ocean SST trends closer to those observed in all models it has been tested in.

Antarctic meltwater input may also have remote impacts, with the potential to explain some of the observed SST trends and model-observation discrepancies in the tropical Pacific. Ma and Wu (2011) demonstrated that adding anomalous Antarctic meltwater in a coupled GCM resulted in surface cooling extending from the Southern Ocean to the tropics. Hwang et al. (2017) found that delayed Southern Ocean warming in a slab-ocean model could drive a tropical La Niña-like SST response via changing the zonal-mean atmospheric heat transport. This Southern Ocean-to-tropics teleconnection has further been supported by a variety of models with anomalous zonal-mean heat fluxes in the Southern Ocean (Kang et al., 2020). More recently, Dong et al. (2022) proposed a two-way atmospheric pathway associated with regional atmospheric circulation instead of zonal-mean heat transport, linking the observed cooling in the tropical eastern Pacific and the southeast Pacific sector of the Southern Ocean. Kim et al. (2022) also found that the inter-model spread in the teleconnection between these two regions is largely determined by differences in the subtropical cloud feedback across models. All of these studies suggest that the observed tropical eastern Pacific cooling may be linked to the observed Southern Ocean cooling, which itself could be a direct response to Antarctic meltwater input.

Antarctic meltwater has been found to reduce projected global warming rates as well (Bronselaer et al., 2018; Sadai et al., 2020; Schloesser et al., 2019). From the standard model of global energy balance (Gregory & Forster, 2008; Gregory et al., 2004, 2015; Raper et al., 2002):

$$N = \lambda T + F = \kappa T, \tag{1}$$

the global-mean near-surface air temperature trend (dT/dt) can be approximated as:

$$dT/dt = \frac{dF/dt}{\kappa - \lambda}, \tag{2}$$

where N is the global-mean energy imbalance (units Wm^{-2}), F is the effective radiative forcing (ERF; units Wm^{-2}), κ is the ocean heat uptake (OHU) efficiency parameter (units $Wm^{-2}K^{-1}$), and λ is the radiative feedback parameter (unit: $Wm^{-2}K^{-1}$, negative for a stable climate). In this zero-layer energy balance model, κ and λ together determine the Earth's surface temperature response to a forcing, with κ representing the efficiency with which heat is absorbed by the ocean and λ representing the efficiency with which heat is radiatively emitted to space at the top of atmosphere (TOA) per degree of global warming. The reduced dT/dt found in previous meltwater simulations has been commonly proposed to arise from an increase in κ, as meltwater cools the Southern Ocean surface but warms the Southern Ocean at depth, making global OHU more efficient (Gregory, 2000; Kirkman & Bitz, 2011). However, it is also possible that meltwater reduces dT/dt by changing λ through the SST pattern effect. Recent studies have found that an SST pattern with enhanced warming in the tropical western Pacific warm pool and cooling in other regions, as recently observed, tends to increase the lower-tropospheric stability and low-cloud cover globally, yielding a more-negative λ and therefore a lower effective climate sensitivity (EffCS; Zhou et al., 2016; Andrews et al., 2018; Dong et al., 2019; Fueglistaler, 2019; Andrews et al., 2022). Given that Antarctic meltwater could produce surface cooling in both the Southern Ocean (due to increased ocean stratification) and the tropical eastern Pacific (due to teleconnections)—an SST pattern closer to the observed—it is possible that some portion of the reduced global warming rate is due to changes in λ via SST pattern effects. A key question is: does Antarctic meltwater primarily influence the warming rate dT/dt through changes in κ or λ?

To better understand the impact of Antarctic meltwater input on transient and near-equilibrium global warming, this study aims to quantify (a) changes in κ and λ caused by Antarctic meltwater input and (b) the respective

impacts of κ and λ changes on the global warming rate. To do that, we employ two sets of published simulations with additional Antarctic meltwater fluxes, the so called "hosing" simulations. One is focused on the recent historical period (leveraging simulations performed by Pauling et al., 2016); the other is focused on the 21st century (leveraging simulations performed by Sadai et al., 2020). Both studies have previously examined the local response to the imposed meltwater forcing, showing an increased Antarctic sea-ice extent and Southern Ocean surface cooling response consistent with other studies. Here we revisit these simulations, focusing on the response of global SST patterns and the global energy budget.

2. Methods

2.1. CESM1 Meltwater Simulations

We analyze two sets of meltwater hosing simulations performed using the fully-coupled CESM1-CAM5 (Neale et al., 2010). The first set (from Pauling et al., 2016) spans the historical period from 1980 to 2013. We hereafter refer to these as the "Historical Hosing" runs, though the simulations apply transient historical radiative forcing until 2005 and Representative Concentration Pathway 8.5 forcing thereafter to be consistent with CESM1 Large Ensemble (LENS) simulations (Kay et al., 2015). This ensemble consists of nine members (we have performed seven more since the publication of Pauling et al. (2016) following the same setup). Each of the nine members has identical radiative forcing and anomalous meltwater forcing, but they are branched from a different LENS ensemble member. The anomalous freshwater input is added at a constant rate of 2000 Gt/yr throughout the simulations, distributed at the front of ice shelves around Antarctica to mimic their basal melt (see Figure 3b of Pauling et al. (2016) for the imposed freshwater distribution, with the ice shelf location derived from the RTopo-1 data set). Note that the amount of imposed freshwater input is chosen as needed to cause significant change in the annual-mean sea-ice area (Pauling et al., 2016) and Southern Ocean surface temperature within CESM1, and this amount is much larger than the observational estimate of 350 $\pm$ 100 Gt/yr (Rye et al., 2014), a caveat we will come back to in the discussion section. We present results from the ensemble-mean of the nine meltwater runs, and compare changes relative to the ensemble-mean of 40 LENS runs that have no additional Antarctic meltwater (results remain the same if we use the mean of the nine LENS members from which the hosing runs were branched).

The other set of simulations (from Sadai et al., 2020) spans the 21st century from 2006 to 2100. We hereafter refer to these as "Future Hosing" runs. This ensemble has one control run and one meltwater hosing run; both are forced by RCP8.5 transient forcing. Although a single ensemble member, the Future Hosing run includes a large freshwater forcing, estimated by an offline ice-sheet model forced by RCP8.5. The total amount of Antarctic freshwater input in the control run (from increasing precipitation only) stays around 0.1 Sv (≈3,154 Gt/yr) throughout the 21st century, whereas that in the Hosing run (accounting for ice-sheet melting) reaches ∼1 Sv (≈31,540 Gt/yr) in 2100. We take the difference between the control run and the Hosing run as the effect of Antarctic meltwater input in this ensemble.

Although using the same model, our Historical and Future Hosing simulations differ in several aspects. First, the Historical Hosing ensemble applies a constant rate of meltwater input while the Future run imposes time-varying meltwater input throughout the simulation. Second, the amount of meltwater input used in the Future simulation is substantially larger than that used in the Historical ensemble. At the end of the 21st century, the imposed meltwater input is nearly 15 times that of the historical meltwater input. Finally, the freshwater forcing applied in the Future simulation includes both liquid meltwater and solid ice (Figure S1a in Supporting Information S1), with the latter used to account for the latent heat (LH) of melting. In contrast, the Historical Hosing simulations only consider liquid meltwater (which is treated as a negative salinity forcing in the model), without accounting for the LH loss from the ocean.

2.2. Global Energy Budget Analysis

For both Historical and Future Hosing simulations, we calculate the OHU efficiency κ and the net radiative feedback λ following the conventional global-energy budget framework expressed in Equation 1 (Gregory et al., 2004, 2015), where $\kappa = dN/dT$, and $\lambda = d(N - F)/dT$. Note that N is taken as the global-mean net TOA radiation imbalance, which is in general equal to the global-mean OHU and therefore can be used to calculate κ. One exception is the Future Hosing run, which includes the LH taken from the ocean to melt the solid ice. These additional heat fluxes can be

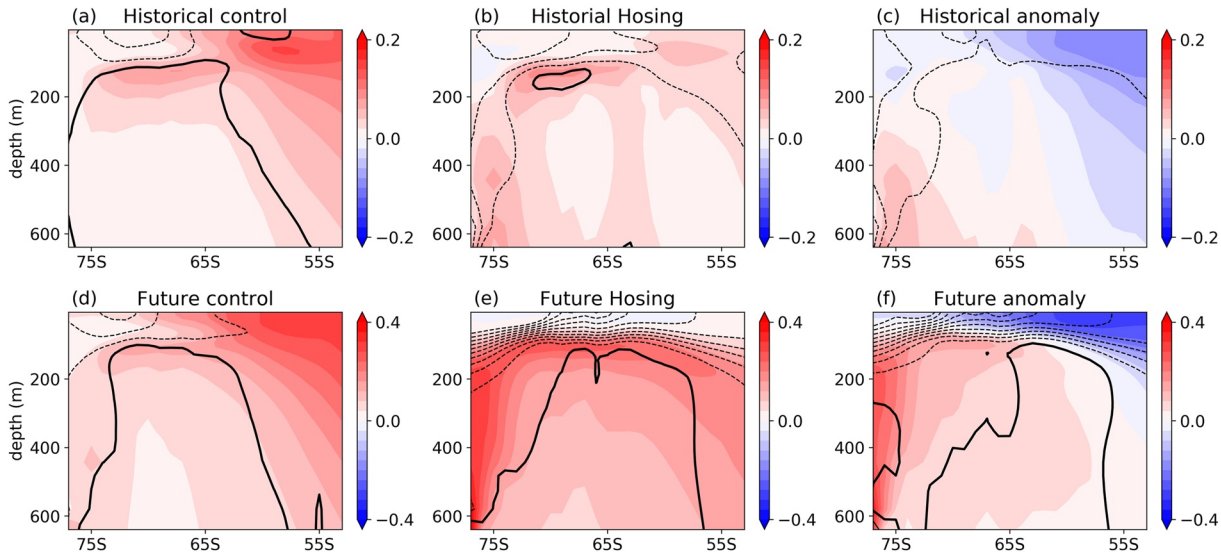

Figure 1. Zonal-mean ocean temperature trends (K/decade; shading) and salinity trends (g/kg/decade; contours) in the Southern Ocean. (a–c) Historical ensemble's control run, hosing run, and the difference (hosing minus control). (d–f) Future ensemble's control run, hosing run, and the difference. Contour interval in (a–c) is 0.01 g/kg/decade and in (d–f) is 0.02 g/kg/decade. Dashed contours denote negative anomalies; zero contours are thickened in all panels. Trends are calculated over 1980–2013 for (a–c) and 2006–2100 for (d–f).

accounted for by subtracting the LH needed to melt all the imposed solid ice from the net TOA radiation imbalance (Figure S1 in Supporting Information S1). We then calculate κ as $d(N - LH)/dT$ for this simulation. The LH of ice melt amounts to approximately 10% of the total global energy imbalance, and thus has a small effect on κ. Importantly, it does not influence the calculation of λ which depends only on TOA radiation. Since our focus in on transient warming, we calculate κ and λ respectively by regressing annual-mean N or $N - F$ against annual-mean T over the time period that the two ensembles span, namely, 1980–2013 for Historical Hosing and 2006–2100 for Future Hosing. We calculate the corresponding EffCS values ($=-F_{2x}/\lambda$, where F_{2x} is the radiative forcing of CO_2 doubling in CESM1), using the estimate of $F_{2x} = 3.88$ Wm^{-2} from Mitevski et al. (2021). EffCS here indicates an estimate of equilibrium climate sensitivity (ECS) using λ from a transient state, under the assumption that λ stays constant to equilibrium; it should be distinguished from the long-term Earth system sensitivity that involves changes in ice sheets operating on millennium timescales (Knutti et al., 2017).

The effective radiative forcing (F) corresponding to these two ensembles is not explicitly available from CESM1 model output. We thus perform an additional fixed-SST simulation to estimate ERF following CMIP6 Radiative Forcing Model Intercomparison Project protocol (Pincus et al., 2016). That is, we carry out a simulation using the atmospheric component of CESM1 (i.e., CAM5), with the same transient historical forcing for 1980–2013 and RCP8.5 forcing for 2006–2100 as used in the coupled CESM1 simulations, while fixing SST and sea-ice concentration at their preindustrial levels. ERF is then estimated as the TOA radiation anomaly of this fixed SST simulation relative to preindustrial levels (Dong et al., 2021; Pincus et al., 2016). All variables (F, N, T) used in this study are annual means.

3. Results

3.1. Local and Remote Temperature Responses to Antarctic Meltwater Input

We begin by analyzing the local response of Southern Ocean zonal-mean temperature and salinity trends (Figure 1). In both ensembles, Antarctic meltwater input causes anomalous surface cooling, subsurface warming, and surface freshening in the Southern Ocean (Figure 1, right column). The Future Hosing run produces stronger responses likely because it imposes a substantially larger amount of meltwater input. Although the LH included in the Future Hosing run could also amplify the Southern Ocean temperature response to meltwater input, this effect is much smaller than the response to the meltwater-induced freshening itself (Figure 2 in Pauling et al., 2017). These local responses are qualitatively consistent with other studies (Bintanja et al., 2013; Bronselaer et al., 2018; Rye et al., 2020), reflecting an increase in upper ocean stratification and a decrease in upward heat transport. The

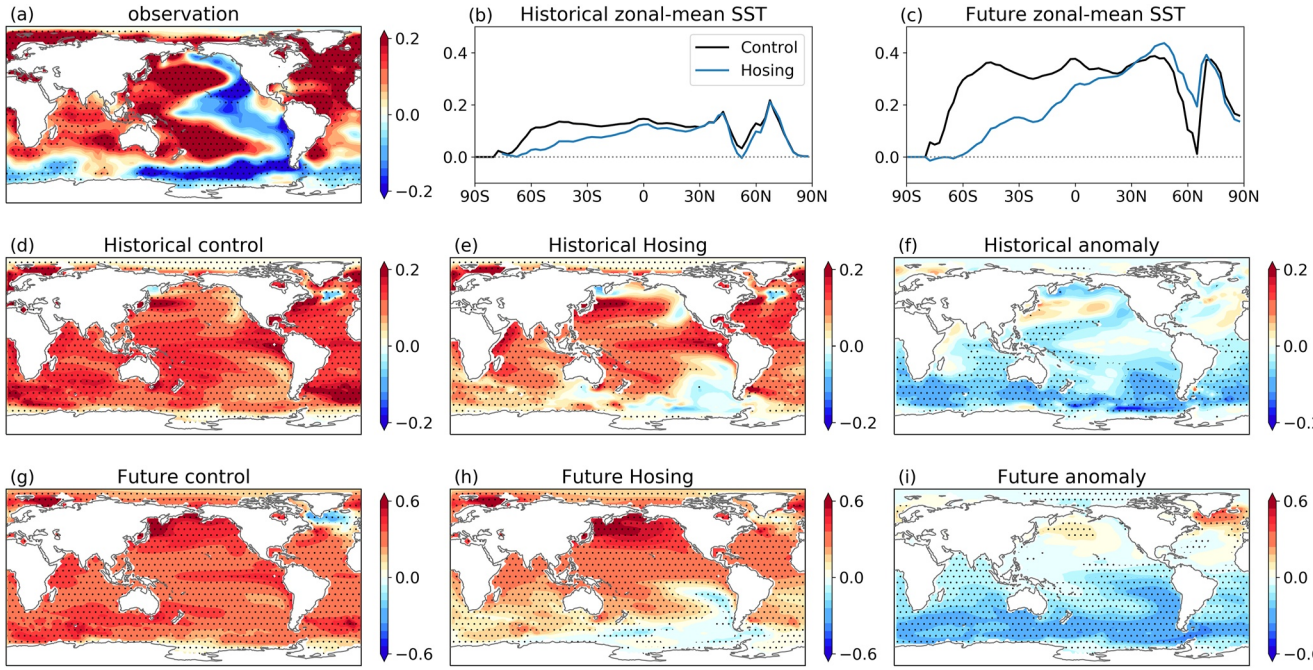

Figure 2. Global patterns of SST trends (K/decade), from (a) ERSSTv5 observations (Huang et al., 2017), (d–f) Historical control, Historical Hosing, and the difference, and (g–i) Future control, Future Hosing, and the difference, respectively. (b–c) Zonal-mean SST trends for the Historical and Future ensemble, respectively. Historical SST trends are calculated over 1980–2013 and Future SST trends are over 2006–2100. Stippling indicates statistically significant linear trends at the 95% level.

magnitude of Southern Ocean temperature and salinity trends in the Historical Hosing simulations is still weaker than that observed (Figure S2 in Supporting Information S1) despite the fact that we imposed such a large amount of meltwater forcing. However, the pattern of those trends becomes qualitatively closer to observations than that simulated without meltwater input. The underestimated Southern Ocean trends in the Hosing simulations may be caused by a too-weak sensitivity to meltwater input in the model (Pauling et al., 2016) or a combined effect with other factors that have contributed to the observed Southern Ocean temperature trends, for example, the strengthening in the Southern Hemisphere midlatitude jet owing to the Antarctic ozone hole (Hartmann, 2022; Kostov et al., 2018). Overall, these results suggest that the lack of realistic Antarctic meltwater input in models may explain some of the model-observation discrepancies in the Southern Ocean.

We next consider the remote SST response to Antarctic meltwater input (Figure 2). In both ensembles, the meltwater-induced Southern Ocean SST cooling extends to lower latitudes in the Southern Hemisphere (Figures 2b and 2c), with the largest cooling occurring in the southeastern Pacific (Figures 2f and 2i). Notably, the Historical Hosing runs with all radiative forcings produce net cooling trends in the southeast Pacific sector of the Southern Ocean and the tropical southeast Pacific (Figure 2e)—the two regions where observations have shown pronounced cooling trends, albeit with a much stronger magnitude than those simulated (Figure 2a). These two regions have also been found to have the strongest teleconnection via an atmospheric pathway, involving subtropical advection near the Andes and tropics-originated Rossby wave dynamics (Dong et al., 2022).

Finally, we consider how Antarctic meltwater influences the global warming rate (Figure 3). In the Historical Hosing runs, the global-mean near-surface air temperature trend dT/dt (over 1980–2013) is reduced by 20%, and in the Future Hosing run dT/dt (over 2006–2100) is reduced by 28% (Table 1). Moreover, the Historical Hosing runs on average produce a dT/dt of 0.16 K/decade, which is more in line with the observed trend of 0.17 K/decade from HadCRUT5 (Morice et al., 2021) than that simulated on average without meltwater input (dT/dt = 0.2 K/decade). This suggests that the lack of Antarctic meltwater in models may explain some of the model biases in historical global-mean warming as well.

In summary, we find that Antarctic meltwater input in CESM1 causes local and remote climate changes that are consistent with previous studies. Accounting for anomalous meltwater input qualitatively reduces model biases in

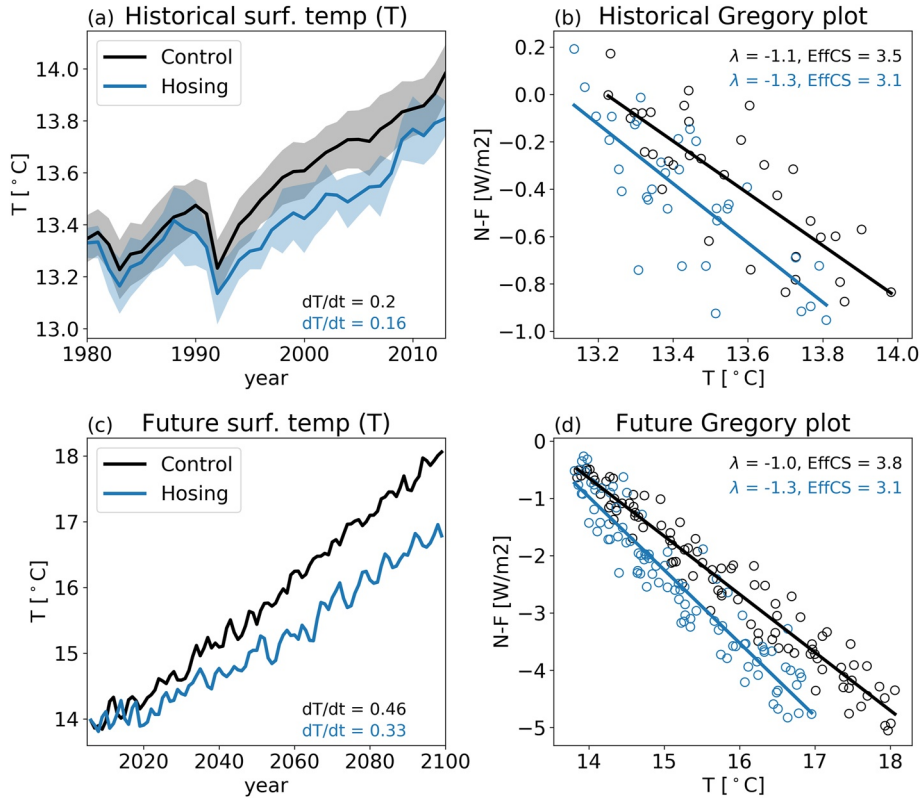

Figure 3. Ensemble-mean global-mean responses to meltwater input in (top) the Historical Hosing ensemble and (bottom) Future Hosing ensemble. (left) Global-mean near-surface air temperatures (T). (right) the Gregory plot (the net TOA radiative response $N - F$ against T). Black and blue denote results of control and hosing runs respectively. Shading in (a) represents ± one standard deviation across ensemble members.

the historical record and also changes the projected warming in the near future. In the following sections we seek to further understand the relative roles of OHU efficiency (κ) and radiative feedback (λ) changes in reducing the global warming rate under meltwater forcing.

3.2. The Response of κ and λ to Antarctic Meltwater Input

Having shown the global surface temperature response to Antarctic meltwater input, next we quantify the changes in κ and λ, two quantities that determine the rate of warming (dT/dt) as expressed by the zero-layer energy balance model (Equation 2).

Table 1
Estimates of Global-Mean Near-Surface Air Temperature Trend (dT/dt), κ, λ, and EffCS for the Simulations Used in This Study

	Historical		Future	
	Control	Hosing	Control	Hosing
dT/dt (K/decade)	0.2	0.16	0.46	0.33
dT/dt estimated by Equation 2 (K/decade)	0.19	0.17	0.46	0.37
dT/dt_κ (K/decade)	–	0.18	–	0.43
dT/dt_λ (K/decade)	–	0.18	–	0.40
κ ($Wm^{-2}K^{-1}$)	1.15	1.34	0.5	0.62
λ ($Wm^{-2}K^{-1}$)	−1.1	−1.25	−1.01	−1.27
EffCS (K)	3.5	3.1	3.9	3.1

We find that the OHU efficiency strengthens in response to Antarctic meltwater: κ increases by 17% in the Historical Hosing ensemble and by 24% in the Future Hosing run (Table 1). The strengthening of κ is not surprising given the changes in the vertical temperature distribution in the Southern Ocean shown in Figure 1, characterized by anomalous surface cooling and subsurface warming, indicating more efficient OHU. The anomalous heat accumulation at depth has been proposed to principally arise from a reduction in upward heat transport, which is a result of either decreased isopycnic temperature gradient (Gregory, 2000; Kirkman & Bitz, 2011) and/or decreased deep ocean convection (Bintanja et al., 2013; Russell & Rind, 1999), as the upper ocean becomes more stratified.

Meanwhile, we find that the net radiative feedback also becomes more stabilizing in the hosing runs: the magnitude of λ increases (more negative λ) by 14% in the Historical Hosing ensemble and by 26% in the Future Hosing run (Figure 3, Table 1). Furthermore, the more-stabilizing radiative feedbacks imply lower effective climate sensitivity: EffCS is reduced from 3.5 to 3.1 K in the Historical Hosing ensemble and from 3.9 to 3.1 K in the Future Hosing run. Although the reduced EffCS values are still higher than the EffCS value of about 2 K estimated from atmospheric model simulations forced by the observed historical SSTs (Andrews et al., 2022), adding meltwater input qualitatively reduces EffCS biases in fully-coupled historical simulations (Dong et al., 2021). We note that λ changes in principle could equivalently be regarded as a result of changes in OHU efficacy arising from changes in the OHU pattern (Lin et al., 2021; Rose et al., 2014; Rugenstein et al., 2016), although this interpretation is complicated by the fact that non-CO_2 forcings may also contribute to feedback changes. In our simulations, the changes in λ are primarily from the Southern Hemisphere (Figure S3 in Supporting Information S1), associated with changes in the low-cloud feedback through the SST pattern effect (Dong et al., 2019; Zhou et al., 2016). In the tropical and subtropical Pacific, the strengthened east-west SST gradient increases lower tropospheric stability, promoting more subtropical low clouds in the eastern Pacific stratocumulus deck (Andrews et al., 2018; Dong et al., 2019; Wood & Bretherton, 2006; Zhou et al., 2016). In the Southern Ocean, the meltwater-induced surface cooling locally yields a more-stable boundary layer, favoring high-coverage stratiform clouds (Atlas et al., 2020; Dong et al., 2019). In both regions, broad increases in low-cloud cover (Figure S3 in Supporting Information S1) lead to stronger reflection of incoming shortwave radiation, and therefore a more-negative cloud feedback.

In summary, both κ and λ strengthen in response to Antarctic meltwater input in our simulations and thus both contribute to slowing the global warming rate. The stronger κ arises mostly from local changes in the depth of Southern Ocean heat storage; the stronger λ arises from local (Southern Ocean) and remote (tropical) changes in cloud feedbacks owing to changes in the SST trend pattern.

3.3. Relative Roles of κ and λ in Changing the Global Warming Rate

Finally, we come back to Equation 2 to quantify the relative roles of κ and λ changes in reducing dT/dt. Although simplified, Equation 2 provides an excellent approximation for the global warming rate (Andrews et al., 2022; Gregory & Forster, 2008; Gregory et al., 2004). Here, we also find that substituting values of dF/dt, κ, and λ into Equation 2 can accurately reproduce values of dT/dt from the corresponding simulations (Table 1). We can thus use the reconstructed values of dT/dt from Equation 2, denoted as dT/dt_{control} and dT/dt_{hosing} for the control runs and the hosing runs respectively, to quantify the relative contributions of changes in κ and λ.

To do so, we first estimate the value of dT/dt that would have occurred if only κ or λ changed while the other remained at the control level, denoted as dT/dt_{κ} or dT/dt_{λ}. We then calculate the change in these estimated dT/dt relative to dT/dt_{control}. Finally, we compare the changes in dT/dt due to changes in λ or κ alone to the total change in dT/dt (calculated as the difference between dT/dt_{hosing} and dT/dt_{control}). We find that in the Historical Hosing ensemble, changes in κ and λ each account for approximately 50% of the total change in dT/dt; while in the Future Hosing run, κ change accounts for only 33% while λ change accounts for 67% of the total change in dT/dt (Table 1). These results suggest that feedback changes can produce reductions in global warming rate that are comparable to or even greater than those produced by OHU efficiency changes. The meltwater-induced reduction in global warming rate has long been thought to arise from more efficient OHU in the Southern Ocean (stronger κ); our results show that Antarctic meltwater input can reduce the global warming rate via changes in radiative feedbacks as well.

4. Discussion and Conclusions

Model-observation discrepancies in the recent historical record call into question our ability to accurately project future warming at both global and regional scales. While many recent studies have shown that the observed tropical SST trends and circulation changes could be influenced by various Southern Ocean forcings through teleconnections (Dong et al., 2022; Hartmann, 2022; Kang et al., 2020; Kim et al., 2022), here we examined the impact of anomalous Antarctic meltwater on tropical SST pattern effects and the global warming rate. Within two sets of meltwater hosing simulations performed using CESM1-CAM5, we find that the transient global warming rate is reduced by Antarctic meltwater input, owing to both a stronger OHU efficiency and a stronger radiative feedback (corresponding to a lower effective climate sensitivity). The strengthening in κ arises mostly from local changes in the depth of Southern Ocean heat storage, while the strengthening in λ arises from both local (Southern Ocean) and remote (tropical) SST changes that enhance negative cloud feedback through the SST pattern effect. Notably, accounting for anomalous Antarctic meltwater input produces a historical SST trend pattern better resembling observations than that simulated without meltwater input. The pattern effect-induced feedback changes contribute about equally to (in Historical Hosing) or twice as much as (in Future Hosing) OHU efficiency changes in reducing the global warming rate. These findings highlight a key role of Antarctic meltwater input in modulating regional and global climates.

Our results, which are based on the use of a single GCM, come with caveats. First, the amount of additional meltwater input needed to cause significant changes has been found to be highly model dependent. Here we applied an amount of Antarctic meltwater (in the Historical Hosing ensemble) to CESM1 approximately five to eight times larger than observational estimates. Although overestimating the observed meltwater amount, our meltwater runs still underestimate the observed surface cooling and freshening over the historical period (c.f. Figure 1b and Figure S2 in Supporting Information S1). This suggests that the local and remote response to the observed Southern Ocean surface freshening in nature may be even stronger than in our simulations, or that other mechanisms have contributed to the observed Southern Ocean surface cooling as well. Second, the extent to which κ changes in response to Antarctic meltwater input may also be model dependent. For instance, it may depend on the Southern Ocean mean state, associated with model representation of deep ocean convection (Cabré et al., 2017). Finally, while our results suggest a key role of the tropical SST pattern effect, the strength of the extratropical-to-tropical teleconnection appears to also be model dependent, with the inter-model spread largely coming from differences in the modeled subtropical cloud feedback (Kim et al., 2022). Thus, different results may arise from model differences in the Southern Ocean (e.g., representation of ocean mean states) and/or in the tropics (e.g., representation of atmospheric radiative feedbacks and teleconnection pathways). The robustness of our findings need to be tested in a range of models to better constrain the impact of Antarctic meltwater on global climate.

Despite these caveats, our results have important implications for understanding historical and future climate change. First, the addition of Antarctic meltwater in the Historical ensemble reduces the ensemble-mean global warming rate from 0.2 to 0.16 K/decade, which is more in line with the observed rate of 0.17 K/decade, albeit with substantially more additional meltwater than observational estimates suggest as discussed earlier. EffCS is also reduced from 3.5 to 3.1 K, which is closer to the EffCS estimate of about 2 K from atmospheric model simulations forced by the observed historical SST pattern (i.e., AMIP simulations) and from observed energy budget constraints (Andrews et al., 2022). Second, with realistic meltwater input, the Future Hosing run projects a muted global warming over the coming century and a lower EffCS value than those simulated without meltwater input. If our results hold in other models, this finding suggests that the near-future warming projections by current GCMs may be overestimated. Furthermore, many studies attribute the recent observed SST trend pattern (with cooling in the tropical eastern Pacific and the Southern Ocean) to internal variability (e.g., the negative phase of Inter-decadal Pacific Oscillation), and therefore hypothesize a reversal of SST trends in these regions to appear in the coming decades (Chung et al., 2022; Watanabe et al., 2021). However, our simulations show that a similar historical SST pattern can arise with sufficient Antarctic meltwater forcing and that this SST pattern can persist into the 21st century in the presence of increasing Antarctic meltwater input.

Additionally, an emergent constraint has recently been proposed linking model simulated historical warming to the model's ECS. Some studies find that models with higher ECS tend to overestimate the observed global-mean warming rate over recent decades (Jiménez-de-la Cuesta & Mauritsen, 2019; Nijsse et al., 2020; Tokarska et al., 2020). Other studies find that even when models reproduce the global-mean warming, the

models with too positive cloud feedback and higher ECS tend to produce less realistic interhemispheric asymmetry in surface warming (Wang et al., 2021). Both suggest that lower ECS values are more likely. However, our simulations show that adding anomalous Antarctic meltwater can reduce model biases by producing a lower global-mean warming rate and an enhanced northern-southern hemispheric temperature asymmetry, more in line with observations (Table S1 in Supporting Information S1). This suggests that model biases in the transient historical warming may be (in part) due to the lack of realistic meltwater forcing, and not necessarily due to model biases in equilibrium response to CO_2 as those emergent constraints assume. Thus, high ECS may be more realistic than previously thought if Antarctic meltwater input has slowed the recent southern hemispheric and global warming rates.

This work has shown a nontrivial impact of Antarctic meltwater input on both regional and global transient warming. Accurately projecting historical and future climate change thus requires improved representation of realistic Antarctic meltwater input and its impacts in GCMs.

Data Availability Statement

The Future Hosing simulations (first published in Sadai et al., 2020) are available at https://doi.org/10.15784/601449. The Historical Hosing ensemble (first published in Pauling et al., 2016) are available at https://doi.org/10.5281/zenodo.7072848. The CESM1 LENS simulations are obtained from https://www.cesm.ucar.edu/community-projects/lens/data-sets.

Acknowledgments
YD was supported by the NOAA Climate and Global Change Postdoctoral Fellowship Program, administered by UCAR's Cooperative Programs for the Advancement of Earth System Science (CPAESS) under award NA210AR4310383. KCA was supported by the National Science Foundation (Grant AGS-1752796), the National Oceanic and Atmospheric Administration MAPP Program (Award NA20OAR4310391), and an Alfred P. Sloan Research Fellowship (Grant FG-2020-13568). The authors acknowledge high-performance computing support from Cheyenne (https://doi.org/10.5065/D6RX99HX) provided by NCAR's Computational and Information Systems Laboratory, sponsored by the National Science Foundation.

References

Andrews, T., Bodas-Salcedo, A., Gregory, J. M., Dong, Y., Armour, K. C., Paynter, D., et al. (2022). On the effect of historical SST patterns on radiative feedback. *Journal of Geophysical Research: Atmospheres*, *127*(18), e2022JD036675. https://doi.org/10.1029/2022jd036675

Andrews, T., Gregory, J. M., Paynter, D., Silvers, L. G., Zhou, C., Mauritsen, T., et al. (2018). Accounting for changing temperature patterns increases historical estimates of climate sensitivity. *Geophysical Research Letters*, *45*(16), 8490–8499. https://doi.org/10.1029/2018gl078887

Armour, K. C., Marshall, J., Scott, J. R., Donohoe, A., & Newsom, E. R. (2016). Southern Ocean warming delayed by circumpolar upwelling and equatorward transport. *Nature Geoscience*, *9*(7), 549–554. https://doi.org/10.1038/ngeo2731

Atlas, R., Bretherton, C. S., Blossey, P. N., Gettelman, A., Bardeen, C., Lin, P., & Ming, Y. (2020). How well do large-eddy simulations and global climate models represent observed boundary layer structures and low clouds over the summertime southern ocean? *Journal of Advances in Modeling Earth Systems*, *12*(11), e2020MS002205. https://doi.org/10.1029/2020ms002205

Bintanja, R., van Oldenborgh, G. J., Drijfhout, S., Wouters, B., & Katsman, C. (2013). Important role for ocean warming and increased ice-shelf melt in Antarctic sea-ice expansion. *Nature Geoscience*, *6*(5), 376–379. https://doi.org/10.1038/ngeo1767

Bronselaer, B., Winton, M., Griffies, S. M., Hurlin, W. J., Rodgers, K. B., Sergienko, O. V., et al. (2018). Change in future climate due to Antarctic meltwater. *Nature*, *564*(7734), 53–58. https://doi.org/10.1038/s41586-018-0712-z

Cabré, A., Marinov, I., & Gnanadesikan, A. (2017). Global atmospheric teleconnections and multidecadal climate oscillations driven by Southern Ocean convection. *Journal of Climate*, *30*(20), 8107–8126. https://doi.org/10.1175/jcli-d-16-0741.1

Chung, E.-S., Kim, S.-J., Timmermann, A., Ha, K.-J., Lee, S.-K., Stuecker, M. F., et al. (2022). Antarctic sea-ice expansion and Southern Ocean cooling linked to tropical variability. *Nature Climate Change*, *12*(5), 461–468. https://doi.org/10.1038/s41558-022-01339-z

De Lavergne, C., Palter, J. B., Galbraith, E. D., Bernardello, R., & Marinov, I. (2014). Cessation of deep convection in the open Southern Ocean under anthropogenic climate change. *Nature Climate Change*, *4*(4), 278–282. https://doi.org/10.1038/nclimate2132

Dong, Y., Armour, K. C., Battisti, D. S., & Blanchard-Wrigglesworth, E. (2022). Two-way teleconnections between the Southern Ocean and the tropical Pacific via a dynamic feedback. *Journal of Climate*, *35*(19), 1–37. https://doi.org/10.1175/jcli-d-22-0080.1

Dong, Y., Armour, K. C., Proistosescu, C., Andrews, T., Battisti, D. S., Forster, P. M., et al. (2021). Biased estimates of equilibrium climate sensitivity and transient climate response derived from historical CMIP6 simulations. *Geophysical Research Letters*, *48*(24), e2021GL095778. https://doi.org/10.1029/2021gl095778

Dong, Y., Proistosescu, C., Armour, K. C., & Battisti, D. S. (2019). Attributing historical and future evolution of radiative feedbacks to regional warming patterns using a Green's function approach: The preeminence of the western Pacific. *Journal of Climate*, *32*(17), 5471–5491. https://doi.org/10.1175/jcli-d-18-0843.1

Durack, P. J. (2015). Ocean salinity and the global water cycle. *Oceanography*, *28*(1), 20–31. https://doi.org/10.5670/oceanog.2015.03

England, M. H., McGregor, S., Spence, P., Meehl, G. A., Timmermann, A., Cai, W., et al. (2014). Recent intensification of wind-driven circulation in the Pacific and the ongoing warming hiatus. *Nature Climate Change*, *4*(3), 222–227. https://doi.org/10.1038/nclimate2106

Fan, T., Deser, C., & Schneider, D. P. (2014). Recent Antarctic sea ice trends in the context of Southern Ocean surface climate variations since 1950. *Geophysical Research Letters*, *41*(7), 2419–2426. https://doi.org/10.1002/2014gl059239

Fueglistaler, S. (2019). Observational evidence for two modes of coupling between sea surface temperatures, tropospheric temperature profile, and shortwave cloud radiative effect in the tropics. *Geophysical Research Letters*, *46*(16), 9890–9898. https://doi.org/10.1029/2019gl083990

Gille, S. T. (2008). Decadal-scale temperature trends in the Southern Hemisphere ocean. *Journal of Climate*, *21*(18), 4749–4765. https://doi.org/10.1175/2008jcli2131.1

Gregory, J. M. (2000). Vertical heat transports in the ocean and their effect on time-dependent climate change. *Climate Dynamics*, *16*(7), 501–515. https://doi.org/10.1007/s003820000059

Gregory, J. M., Andrews, T., & Good, P. (2015). The inconstancy of the transient climate response parameter under increasing CO_2. *Philosophical Transactions of the Royal Society A: Mathematical, Physical & Engineering Sciences*, *373*(2054), 20140417. https://doi.org/10.1098/rsta.2014.0417

Gregory, J. M., & Forster, P. (2008). Transient climate response estimated from radiative forcing and observed temperature change. *Journal of Geophysical Research*, *113*(D23), D23105. https://doi.org/10.1029/2008jd010405

Gregory, J. M., Ingram, W. J., Palmer, M. A., Jones, G. S., Stott, P. A., Thorpe, R. B., et al. (2004). A new method for diagnosing radiative forcing and climate sensitivity. *Geophysical Research Letters*, *31*(3), L03205. https://doi.org/10.1029/2003gl018747

Hartmann, D. L. (2022). The Antarctic ozone hole and the pattern effect on climate sensitivity. *Proceedings of the National Academy of Sciences*, *119*(35), e2207889119. https://doi.org/10.1073/pnas.2207889119

Huang, B., Thorne, P. W., Banzon, V. F., Boyer, T., Chepurin, G., Lawrimore, J. H., et al. (2017). Extended reconstructed sea surface temperature, version 5 (ERSSTv5): Upgrades, validations, and intercomparisons. *Journal of Climate*, *30*(20), 8179–8205. https://doi.org/10.1175/jcli-d-16-0836.1

Hwang, Y.-T., Xie, S.-P., Deser, C., & Kang, S. M. (2017). Connecting tropical climate change with southern ocean heat uptake. *Geophysical Research Letters*, *44*(18), 9449–9457. https://doi.org/10.1002/2017gl074972

Jiménez-de-la Cuesta, D., & Mauritsen, T. (2019). Emergent constraints on Earth's transient and equilibrium response to doubled CO_2 from post-1970s global warming. *Nature Geoscience*, *12*(11), 902–905. https://doi.org/10.1038/s41561-019-0463-y

Kang, S. M., Xie, S.-P., Shin, Y., Kim, H., Hwang, Y.-T., Stuecker, M. F., et al. (2020). Walker circulation response to extratropical radiative forcing. *Science Advances*, *6*(47), eabd3021. https://doi.org/10.1126/sciadv.abd3021

Kay, J. E., Deser, C., Phillips, A., Mai, A., Hannay, C., Strand, G., et al. (2015). The community Earth system model (CESM) large ensemble project: A community resource for studying climate change in the presence of internal climate variability. *Bulletin of the American Meteorological Society*, *96*(8), 1333–1349. https://doi.org/10.1175/bams-d-13-00255.1

Kim, H., Kang, S. M., Kay, J. E., & Xie, S.-P. (2022). Subtropical clouds key to Southern Ocean teleconnections to the tropical Pacific. *Proceedings of the National Academy of Sciences*, *119*(34), e2200514119. https://doi.org/10.1073/pnas.2200514119

Kirkman, C. H., & Bitz, C. M. (2011). The effect of the sea ice freshwater flux on Southern Ocean temperatures in CCSM3: Deep-ocean warming and delayed surface warming. *Journal of Climate*, *24*(9), 2224–2237. https://doi.org/10.1175/2010jcli3625.1

Knutti, R., Rugenstein, M. A., & Hegerl, G. C. (2017). Beyond equilibrium climate sensitivity. *Nature Geoscience*, *10*(10), 727–736. https://doi.org/10.1038/ngeo3017

Kostov, Y., Ferreira, D., Armour, K. C., & Marshall, J. (2018). Contributions of greenhouse gas forcing and the Southern Annular Mode to historical Southern Ocean surface temperature trends. *Geophysical Research Letters*, *45*(2), 1086–1097. https://doi.org/10.1002/2017gl074964

Lee, S., L'Heureux, M., Wittenberg, A. T., Seager, R., O'Gorman, P. A., & Johnson, N. C. (2022). On the future zonal contrasts of equatorial Pacific climate: Perspectives from observations, simulations, and theories. *NPJ Climate and Atmospheric Science*, *5*(1), 1–15. https://doi.org/10.1038/s41612-022-00301-2

Lin, Y.-J., Hwang, Y.-T., Lu, J., Liu, F., & Rose, B. E. (2021). The dominant contribution of Southern Ocean heat uptake to time-evolving radiative feedback in CESM. *Geophysical Research Letters*, *48*(9), e2021GL093302. https://doi.org/10.1029/2021gl093302

Luo, J.-J., Wang, G., & Dommenget, D. (2018). May common model biases reduce CMIP5's ability to simulate the recent Pacific la Niña-like cooling? *Climate Dynamics*, *50*(3), 1335–1351. https://doi.org/10.1007/s00382-017-3688-8

Ma, H., & Wu, L. (2011). Global teleconnections in response to freshening over the Antarctic ocean. *Journal of Climate*, *24*(4), 1071–1088. https://doi.org/10.1175/2010jcli3634.1

McGregor, S., Stuecker, M. F., Kajtar, J. B., England, M. H., & Collins, M. (2018). Model tropical Atlantic biases underpin diminished Pacific decadal variability. *Nature Climate Change*, *8*(6), 493–498. https://doi.org/10.1038/s41558-018-0163-4

Mitevski, I., Orbe, C., Chemke, R., Nazarenko, L., & Polvani, L. M. (2021). Non-monotonic response of the climate system to abrupt CO_2 forcing. *Geophysical Research Letters*, *48*(6), e2020GL090861. https://doi.org/10.1029/2020gl090861

Morice, C. P., Kennedy, J. J., Rayner, N. A., Winn, J., Hogan, E., Killick, R., et al. (2021). An updated assessment of near-surface temperature change from 1850: The HADCRUT5 data set. *Journal of Geophysical Research: Atmospheres*, *126*(3), e2019JD032361. https://doi.org/10.1029/2019jd032361

Neale, R. B., Chen, C.-C., Gettelman, A., Lauritzen, P. H., Park, S., Williamson, D. L., et al. (2010). Description of the NCAR community atmosphere model (CAM 5.0). *NCAR Tech. Note NCAR/TN-486+ STR*, *1*(1), 1–12.

Nijsse, F. J., Cox, P. M., & Williamson, M. S. (2020). Emergent constraints on transient climate response (TCR) and equilibrium climate sensitivity (ECS) from historical warming in CMIP5 and CMIP6 models. *Earth System Dynamics*, *11*(3), 737–750. https://doi.org/10.5194/esd-11-737-2020

Park, W., & Latif, M. (2019). Ensemble global warming simulations with idealized Antarctic meltwater input. *Climate Dynamics*, *52*(5), 3223–3239. https://doi.org/10.1007/s00382-018-4319-8

Parkinson, C. L. (2019). A 40-y record reveals gradual Antarctic sea ice increases followed by decreases at rates far exceeding the rates seen in the Arctic. *Proceedings of the National Academy of Sciences*, *116*(29), 14414–14423. https://doi.org/10.1073/pnas.1906556116

Pauling, A. G., Bitz, C. M., Smith, I. J., & Langhorne, P. J. (2016). The response of the Southern Ocean and Antarctic sea ice to freshwater from ice shelves in an Earth system model. *Journal of Climate*, *29*(5), 1655–1672. https://doi.org/10.1175/jcli-d-15-0501.1

Pauling, A. G., Smith, I. J., Langhorne, P. J., & Bitz, C. M. (2017). Time-dependent freshwater input from ice shelves: Impacts on Antarctic sea ice and the Southern Ocean in an Earth System Model. *Geophysical Research Letters*, *44*(20), 10–454. https://doi.org/10.1002/2017gl075017

Pincus, R., Forster, P. M., & Stevens, B. (2016). The radiative forcing model Intercomparison project (RFMIP): Experimental protocol for CMIP6. *Geoscientific Model Development*, *9*(9), 3447–3460. https://doi.org/10.5194/gmd-9-3447-2016

Purich, A., England, M. H., Cai, W., Sullivan, A., & Durack, P. J. (2018). Impacts of broad-scale surface freshening of the Southern Ocean in a coupled climate model. *Journal of Climate*, *31*(7), 2613–2632. https://doi.org/10.1175/jcli-d-17-0092.1

Raper, S. C., Gregory, J. M., & Stouffer, R. J. (2002). The role of climate sensitivity and ocean heat uptake on AOGCM transient temperature response. *Journal of Climate*, *15*(1), 124–130. https://doi.org/10.1175/1520-0442(2002)015<0124:trocsa>2.0.co;2

Roach, L. A., Dörr, J., Holmes, C. R., Massonnet, F., Blockley, E. W., Notz, D., et al. (2020). Antarctic sea ice area in CMIP6. *Geophysical Research Letters*, *47*(9), e2019GL086729. https://doi.org/10.1029/2019gl086729

Rose, B. E., Armour, K. C., Battisti, D. S., Feldl, N., & Koll, D. D. (2014). The dependence of transient climate sensitivity and radiative feedbacks on the spatial pattern of ocean heat uptake. *Geophysical Research Letters*, *41*(3), 1071–1078. https://doi.org/10.1002/2013gl058955

Rugenstein, M. A., Caldeira, K., & Knutti, R. (2016). Dependence of global radiative feedbacks on evolving patterns of surface heat fluxes. *Geophysical Research Letters*, *43*(18), 9877–9885. https://doi.org/10.1002/2016gl070907

Russell, G. L., & Rind, D. (1999). Response to CO_2 transient increase in the GISS coupled model: Regional coolings in a warming climate. *Journal of Climate*, *12*(2), 531–539. https://doi.org/10.1175/1520-0442(1999)012<0531:rtctii>2.0.co;2

Rye, C. D., Marshall, J., Kelley, M., Russell, G., Nazarenko, L. S., Kostov, Y., et al. (2020). Antarctic glacial melt as a driver of recent Southern Ocean climate trends. *Geophysical Research Letters*, *47*(11), e2019GL086892. https://doi.org/10.1029/2019gl086892

Rye, C. D., Naveira Garabato, A. C., Holland, P. R., Meredith, M. P., George Nurser, A., Hughes, C. W., et al. (2014). Rapid sea-level rise along the Antarctic margins in response to increased glacial discharge. *Nature Geoscience*, *7*(10), 732–735. https://doi.org/10.1038/ngeo2230

Sadai, S., Condron, A., DeConto, R., & Pollard, D. (2020). Future climate response to Antarctic Ice Sheet melt caused by anthropogenic warming. *Science Advances*, *6*(39), eaaz1169. https://doi.org/10.1126/sciadv.aaz1169

Schloesser, F., Friedrich, T., Timmermann, A., DeConto, R. M., & Pollard, D. (2019). Antarctic iceberg impacts on future Southern Hemisphere climate. *Nature Climate Change*, *9*(9), 672–677. https://doi.org/10.1038/s41558-019-0546-1

Seager, R., Cane, M., Henderson, N., Lee, D.-E., Abernathey, R., & Zhang, H. (2019). Strengthening tropical Pacific zonal sea surface temperature gradient consistent with rising greenhouse gases. *Nature Climate Change*, *9*(7), 517–522. https://doi.org/10.1038/s41558-019-0505-x

Seager, R., Henderson, N., & Cane, M. (2022). Persistent discrepancies between observed and modeled trends in the tropical Pacific Ocean. *Journal of Climate*, *35*(14), 1–41. https://doi.org/10.1175/jcli-d-21-0648.1

Swart, N., & Fyfe, J. (2013). The influence of recent Antarctic ice sheet retreat on simulated sea ice area trends. *Geophysical Research Letters*, *40*(16), 4328–4332. https://doi.org/10.1002/grl.50820

Takahashi, C., & Watanabe, M. (2016). Pacific trade winds accelerated by aerosol forcing over the past two decades. *Nature Climate Change*, *6*(8), 768–772. https://doi.org/10.1038/nclimate2996

Tokarska, K. B., Stolpe, M. B., Sippel, S., Fischer, E. M., Smith, C. J., Lehner, F., & Knutti, R. (2020). Past warming trend constrains future warming in CMIP6 models. *Science Advances*, *6*(12), eaaz9549. https://doi.org/10.1126/sciadv.aaz9549

Wang, C., Soden, B. J., Yang, W., & Vecchi, G. A. (2021). Compensation between cloud feedback and aerosol-cloud interaction in CMIP6 models. *Geophysical Research Letters*, *48*(4), e2020GL091024. https://doi.org/10.1029/2020gl091024

Watanabe, M., Dufresne, J.-L., Kosaka, Y., Mauritsen, T., & Tatebe, H. (2021). Enhanced warming constrained by past trends in equatorial Pacific sea surface temperature gradient. *Nature Climate Change*, *11*(1), 33–37. https://doi.org/10.1038/s41558-020-00933-3

Wills, R. C. J., Dong, Y., Proistosecu, C., Armour, K. C., & Battisti, D. S. (2022). Systematic climate model biases in the large-scale patterns of recent sea-surface temperature and sea-level pressure change. *Geophysical Research Letters*, *49*(17), e2022GL100011. https://doi.org/10.1029/2022gl100011

Wood, R., & Bretherton, C. S. (2006). On the relationship between stratiform low cloud cover and lower-tropospheric stability. *Journal of Climate*, *19*(24), 6425–6432. https://doi.org/10.1175/jcli3988.1

Zhou, C., Zelinka, M. D., & Klein, S. A. (2016). Impact of decadal cloud variations on the Earth's energy budget. *Nature Geoscience*, *9*(12), 871–874. https://doi.org/10.1038/ngeo2828

References From the Supporting Information

Good, S. A., Martin, M. J., & Rayner, N. A. (2013). En4: Quality controlled ocean temperature and salinity profiles and monthly objective analyses with uncertainty estimates. *Journal of Geophysical Research: Oceans*, *118*(12), 6704–6716. https://doi.org/10.1002/2013jc009067